that adipocytes are normally differentiated in apoE$^{-/-}$;Ay/+ mice in vivo.

Adenoviral apoE replenishment induced obesity and diabetes in genetically obese mice. To confirm that the metabolic phenotypes observed in apoE$^{-/-}$;Ay/+ mice were, in fact, mediated by apoE deficiency, we examined metabolic effects of adenovirus-mediated apoE expression in the livers of apoE$^{-/-}$;Ay/+ mice. Replenishment of apoE protein (human apoE3) resulted in markedly decreased plasma cholesterol, triglyceride, and FFA levels (Supplemental Fig. 2*A* [online appendix]), indicating functional expression of apoE. HPLC analyses of plasma lipid profiles revealed that adenoviral replenishment of apoE protein in apoE$^{-/-}$;Ay/+ mice markedly decreased the chylomicron and VLDL fractions (Supplemental Fig. 2*B* [online appendix]).

Increases in body weight for 7 days after adenoviral administration were significantly greater with the apoE adenovirus than with the LacZ control adenovirus (Fig. 4*A*). Liver weights tended to be increased (Fig. 4*B*), and those of brown adipose (Fig. 4*C*) and epididymal, mesenteric, and retroperitoneal white adipose (Fig. 4*D*) tissues were significantly increased with apoE adenoviral administration. Histological analyses revealed that apoE replenishment increased sizes of brown (Fig. 4*E* and *F*) and white (Fig. 4*G* and *H*) adipocytes. In addition, glucose tolerance tests revealed that apoE replenishment worsened glucose tolerance in apoE$^{-/-}$;Ay/+ mice (Fig. 4*I*). These findings show clearly that circulating apoE contributes to increased adiposity and the glucose intolerance associated with obesity. Furthermore, plasma leptin levels were significantly increased on day 7 after adenoviral administration. TNF-α and adiponectin levels tended to be increased and decreased, respectively (Fig. 4*J*), suggesting that circulating apoEs are involved in obesity-induced alterations in adipocytokine levels.

ApoE occurs in three major isoforms (apoE2, -E3, and -E4) in humans. ApoE3, the most common isoform, is considered to be the wild type. To compare the roles of the three human apoE isoforms in obesity and diabetes, recombinant adenoviruses encoding human apoE2 and -E4 as well as apoE3 were injected into apoE$^{-/-}$;Ay/+ mice. Administration of these apoE adenoviruses resulted in similar expression amounts of apoE proteins (data not shown), and similar increases in body weights (Supplemental Fig. 3*A* [online appendix]) and blood glucose levels (Supplemental Fig. 3*B* [online appendix]). These findings suggest that the three apoE isoforms contribute similarly to fat accumulation and glucose tolerance.

ApoE-less VLDL was uptaken into adipocytes, and the liver was impaired. Why does apoE deficiency inhibit obesity in genetically obese mice? We next examined the uptake of β-VLDL, with or without apoE, into fully differentiated 3T3-L1 adipocytes. β-VLDL obtained from apoE$^{-/-}$ mice was labeled with DiI, followed by incubation with or without recombinant human apoE3. As shown in Fig. 5*A*, uptake of apoE-deficient VLDL was markedly lower, by 85%, than that of apoE-positive (after incubation with human apoE3) VLDL. These findings suggest that impaired VLDL uptake into adipocytes contributes to decreased adiposity in apoE$^{-/-}$;Ay/+ mice. Thus, VLDL uptake into adipocytes is likely to play a role in excess fat deposition and, thereby, in the development of diabetes associated with obesity.

ApoE deficiency reportedly reduces hepatic VLDL secretion, resulting in fatty liver findings (11). In our model as well, hepatic triglyceride secretion was inhibited in apoE$^{-/-}$;Ay/+ mice compared with apoE$^{+/+}$;Ay/+ mice, by 48% (Fig. 5*B*). However, interestingly, apoE$^{-/-}$;Ay/+ mice displayed less fat accumulation in the liver than apoE$^{+/+}$;Ay/+ mice (Fig. 1*D–F*). To elucidate the underlying mechanism, we examined β-VLDL uptake into the liver. Fluorescence-labeled β-VLDL, with or without apoE, was intravenously injected into wild-type C57BL/6 mice. Fluorescence values in the liver were then measured. Uptake of apoE-deficient β-VLDL was markedly lower, by 49%, than that of apoE-positive VLDL (Fig. 5*C*). Thus, despite decreased secretion, decreased β-VLDL uptake with apoE deficiency may contribute to prevention of hepatic steatosis. Therefore, apoE is likely to be involved in excess fat uptake into hepatocytes as well as adipocytes. Taken together with the findings that adenoviral apoE replenishment decreased the VLDL fraction (Supplemental Fig. 2*B* [online appendix]), our results indicate that apoE-dependent VLDL transport into tissues, including the liver and adipose tissue, is involved in the development of obesity, resulting in glucose intolerance and insulin resistance.

ApoE deficiency decreased food intake and increased energy expenditure in genetically obese mice. Next, to elucidate the systemic mechanism underlying the obesity prevention associated with apoE deficiency, we first measured food intakes in apoE$^{+/+}$;Ay/+ and apoE$^{-/-}$;Ay/+ mice. Interestingly, apoE deficiency in Ay mice significantly suppressed food intake (Fig. 5*D*). Then, to eliminate the secondary effects of reduced food intake in apoE$^{-/-}$;Ay/+ mice, ApoE$^{+/+}$;Ay/+ mice were allotted the same amounts of food consumption as apoE$^{-/-}$;Ay/+ mice, followed by weight measurement and glucose tolerance testing. Pair-feeding blunted the body weight increments in apoE$^{+/+}$;Ay/+ mice, while the weights of pair-fed apoE$^{+/+}$;Ay/+ mice were significantly greater than those of apoE$^{-/-}$;Ay/+ mice (Fig. 5*E*). ApoE$^{-/-}$;Ay/+ mice exhibited better glucose tolerance than pair-fed apoE$^{+/+}$;Ay/+ mice (Fig. 5*F*). Thus, the inhibition of obesity and glucose intolerance by apoE deficiency is not attributable solely to decreased food intake.

Next, we measured basal metabolic rates. As shown in Fig. 5*G*, resting oxygen consumption in both the light and the dark phase at 5 weeks of age was significantly greater in apoE$^{-/-}$;Ay/+ than in apoE$^{+/+}$;Ay/+ mice. Taken together with the pair-feeding experiment results, these findings show that decreased food intake and increased energy expenditure both contribute to the prevention of obesity and insulin resistance with apoE deficiency and that apoE is involved in regulation of energy metabolism.

DISCUSSION

To examine the effects of apoE deficiency on insulin resistance associated with obesity, apoE$^{-/-}$ mice were interbred with KK-Ay mice. ApoE$^{-/-}$;Ay/+ mice showed resistance to the development of obesity and glucose intolerance. Insulin sensitivity was markedly greater in apoE$^{-/-}$;Ay/+ than in apoE$^{+/+}$;Ay/+ mice. Recently, several attempts to induce obesity in apoE$^{-/-}$ mice have been reported, but the results have been somewhat controversial (12–14). In the present study, in addition to inhibition of adiposity and insulin resistance with apoE deficiency, adenoviral apoE replenishment reversed inhibition of obesity and glucose intolerance. These findings directly demonstrate apoE involvement in the development of obesity and obesity-related disorders of glucose metabolism and insulin sensitivity. Chiba et al. (14) previously reported

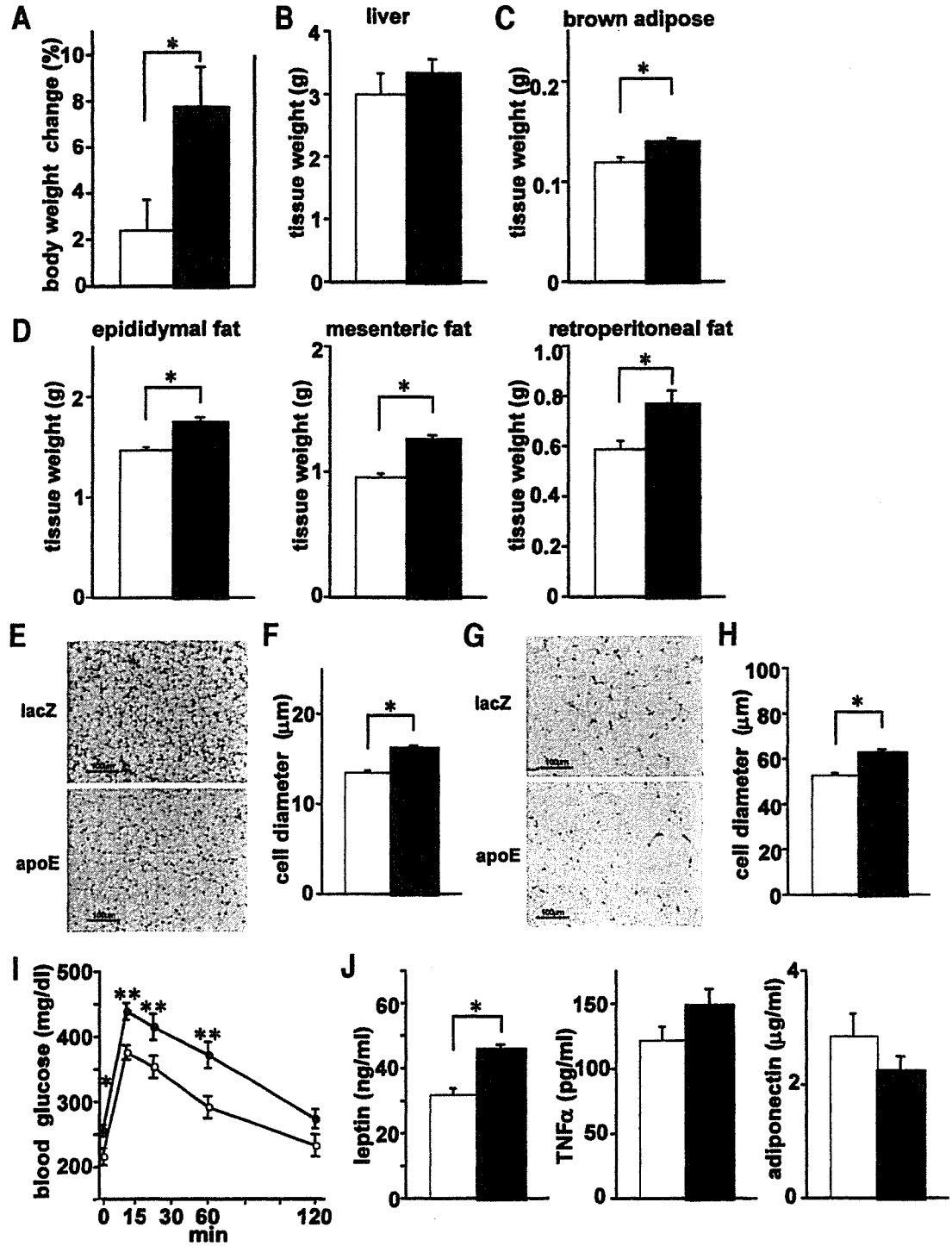

FIG. 4. Adenoviral apoE replenishment induced obesity and diabetes in genetically obese mice. ApoE$^{-/-}$;Ay/+ mice were intravenously administered LacZ (□ or ○) or apoE (■ or ●) adenovirus at 10 weeks of age after 4 weeks of high-fat loading. *A*: Body weight changes for 7 days after adenoviral administration were examined. *B–D*: Weights of the liver (*B*) and brown adipose (*C*) as well as white adipose (*D*: *left*, epididymal fat; *middle*, mesenteric fat; *right*, retroperitoneal fat) tissues were determined on day 7 after adenoviral injection (n = 6 per group). *E–H*: Histological findings of brown adipose (*E* and *F*) and mesenteric white adipose (*G* and *H*) tissues. Representative hematoxylin-eosin stained tissue samples are presented (*E* and *G*). Cell diameters were measured in these tissues (*F* and *H*). *I*: Glucose tolerance tests were performed on day 7 after adenoviral injection (n = 5–8 per group). *J*: Plasma adipocytokine levels (*left*, leptin; *middle*, TNF-α; *right*, adiponectin) were assayed on day 7 after adenoviral injection (n = 5–8 per group). Data are presented as means ± SE. *P < 0.05, **P < 0.01 by the unpaired t test.

that *ob/ob*;apoE$^{-/-}$ mice are also resistant to obesity. They attributed decreased adiposity in *ob/ob*;apoE$^{-/-}$ mice to impaired adipocyte differentiation based on in vitro findings that expression levels of aP2 and peroxisome proliferator–activated receptor-γ were markedly lower when bone marrow stromal cells and 3T3-L1 cells were cultured with apoE-less VLDL. However, in the present study, adipocytes in apoE$^{-/-}$;Ay/+ mice expressed these adipocyte-related proteins normally in vivo. Furthermore, apoE$^{-/-}$;Ay/+ mice showed better insulin sensitivity and less hepatic lipid accumulation, accompanied by improved adipocytokine profiles, than apoE$^{+/+}$;Ay/+ mice. Thus,

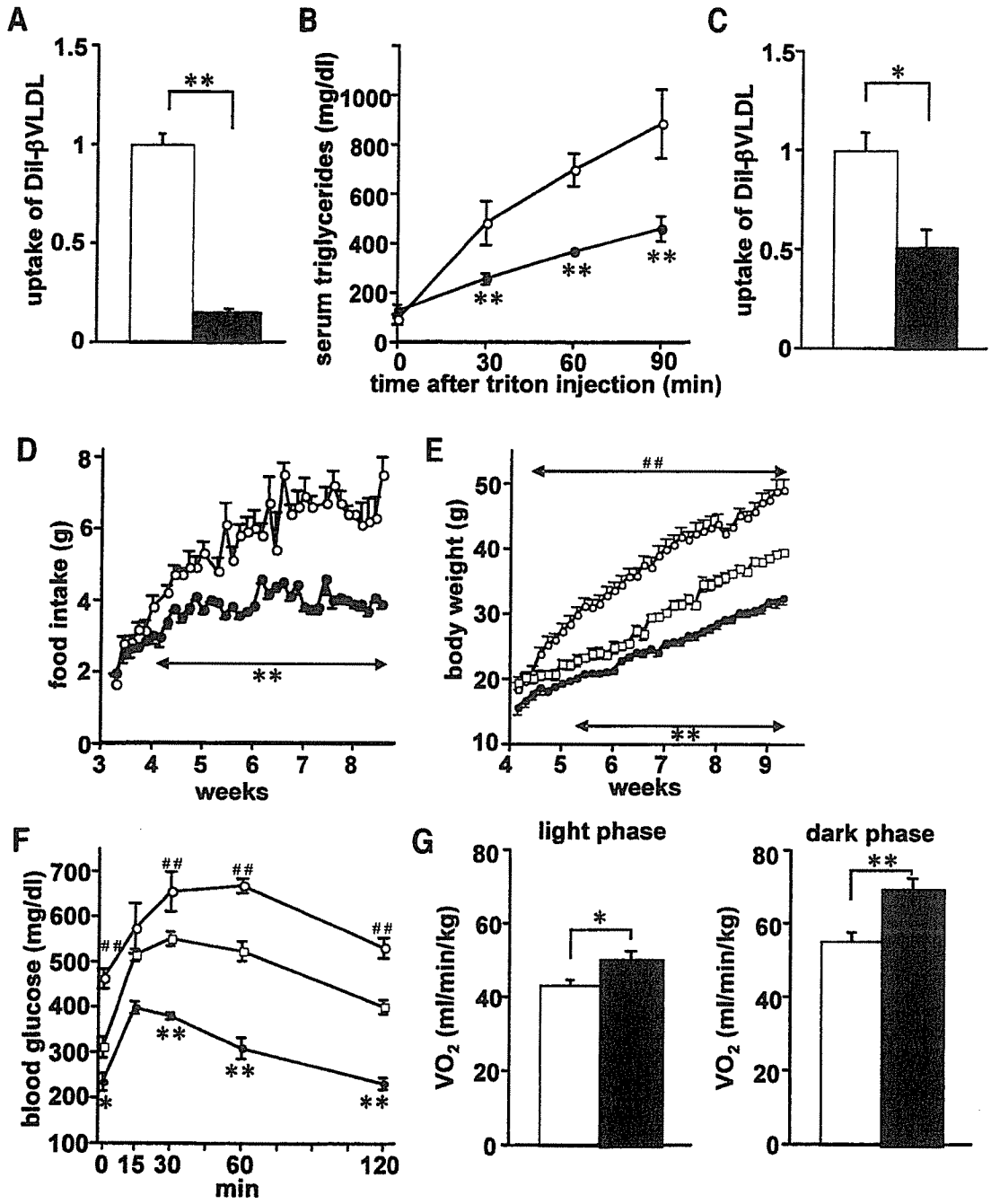

FIG. 5. ApoE deficiency inhibited β-VLDL uptake into adipocytes and the liver, decreased food intake, and increased energy expenditure. *A*: Uptakes of fluorescence-labeled β-VLDL, with (□) or without (■) apoE, into cultured adipocytes were measured. β-VLDL was isolated from apoE$^{-/-}$ mouse sera, followed by labeling with DiI and pretreatment with or without human recombinant apoE3. Fully differentiated 3T3-L1 adipocytes were incubated with apoE-positive or apoE-less β-VLDL for 8 h, followed by measurement of fluorescence uptake into adipocytes. Data are presented as the relative amounts of β-VLDL uptake compared with apoE-positive β-VLDL uptake (n = 6 per group). *B*: Triglyceride secretion rates from the liver after administration of Triton WR-1339 were measured in 11-week-old apoE$^{+/+}$;Ay/+ (○) and apoE$^{-/-}$;Ay/+ (●) mice fed a high-fat diet for 5 weeks. *C*: Hepatic uptake of β-VLDL with or without apoE. Fluorescence-labeled β-VLDL with or without apoE was intravenously injected into 11-week-old apoE$^{+/+}$;Ay/+ mice fed a high-fat diet for 5 weeks, followed by measurement of fluorescence levels in the liver 30 min after injection. Data are presented as the relative amounts of β-VLDL uptake compared with apoE-positive β-VLDL uptake (n = 4 per group). *D*: Daily food intake amounts from weaning through 8 weeks of age are presented. *E* and *F*: ApoE$^{+/+}$;Ay/+ mice were allotted into two groups at 4 weeks of age, and one group of apoE$^{+/+}$;Ay/+mice was given their daily food allotments based on the previous days' consumption by apoE$^{-/-}$;Ay/+ littermate mice. Body weights (*E*) were determined and glucose tolerance tests (*F*) were performed in apoE$^{+/+}$;Ay/+ mice (○), pair-fed apoE$^{+/+}$;Ay/+ mice (□), and apoE$^{-/-}$;Ay/+ mice (●) (n = 6–8 per group). *G*: Resting oxygen consumption in the light and dark phases was measured at 5 weeks of age with open-circuit indirect calorimetry. n = 4 per group. Data are presented as means ± SE. *P < 0.05, **P < 0.01 by the unpaired t test. In *E* and *F* ##P < 0.01 for pair-feeding apoE$^{+/+}$;Ay/+ mice versus apoE$^{+/+}$;Ay/+ mice; *P < 0.05, **P < 0.01 for pair-feeding apoE$^{+/+}$;Ay/+ mice versus apoE$^{-/-}$;Ay/+ mice, by one-way ANOVA.

decreased adiposity and improved insulin sensitivity in apoE$^{-/-}$;Ay/+ mice can be explained by factors other than adipocyte differentiation.

While body weight and adiposity were similar in young apoE$^{-/-}$ and apoE$^{+/+}$ mice, apoE deficiency ameliorated obesity and insulin resistance under obesity-inducing con-

ditions, such as aging, genetic susceptibility, and dietary loading, suggesting that apoE is involved in obesity development, i.e., excess fat accumulation, while being less involved in basal fat accumulation. Lack of apoE in β-VLDL markedly impaired β-VLDL transport into adipocytes. ApoE is an important component of VLDL. There are several receptors, including VLDL receptor (VLDLR) and LDL receptor–related protein, which recognize VLDL in an apoE-dependent manner (22). Among them, VLDLRs reportedly have similar affinities for apoE2, -E3, and -E4 isoforms (29). In addition, VLDLR-deficient mice reportedly exhibit obesity resistance with high-fat chow loading (30). Taken together with our findings that replenishment of apoE2, -E3, and -E4 isoforms contributes similarly to fat accumulation and glucose tolerance in apoE$^{-/-}$;Ay/+ mice, the apoE-VLDLR interaction plays an important role in the development of obesity. Furthermore, it is well known that high levels of plasma VLDL are associated with obesity and type 2 diabetes (31). Thus, receptor-mediated VLDL transport into adipocytes in an apoE-dependent manner is involved mainly in excess lipid uptake into adipocytes. Lipid uptake, required for adipocyte differentiation and metabolic activities, might be mediated mainly by apoE-independent lipid transport pathways or de novo lipid synthesis in adipocytes.

In addition, transport of apoE-deficient β-VLDL into the liver was markedly impaired compared with that of apoE-positive β-VLDL. Despite decreased triglyceride secretion, apoE deficiency decreased hepatic fat accumulation in Ay, but not in wild-type, mice (11). Hepatic expressions of SREBP1c and fatty acid synthase were similar in apoE$^{-/-}$;Ay/+ and apoE$^{+/+}$;Ay/+ mice (data not shown), suggesting no apparent decrease in hepatic fatty acid synthesis in apoE$^{-/-}$;Ay/+ mice. These findings suggest that apoE-dependent uptake of β-VLDL into hepatocytes is involved in the development of hepatic steatosis in Ay mice. The machinery that transports β-VLDL into the liver, including the receptor(s) playing a major role, is a potential target for elucidating the mechanism underlying hepatic steatosis.

Intriguingly, in apoE$^{-/-}$;Ay/+ mice, food intake was decreased and energy expenditure enhanced compared with apoE$^{+/+}$;Ay/+ mice. Pair-feeding experiments revealed that both these phenomena result in obesity resistance in apoE$^{-/-}$;Ay/+ mice. There appear to be several possible explanations for these alterations in energy metabolism. First, hyperlipidemia induced by apoE deficiency might contribute to decreased food intake and increased energy expenditure. However, LDLR$^{-/-}$ mice, which also exhibit hyperlipidemia, reportedly become more obese and diabetic in response to high-fat and high-carbonate diets than wild-type mice (13). In addition, food intake was similar in LDLR$^{-/-}$ mice and LDLR$^{+/+}$ mice (13). Therefore, although hyperlipidemia is more severe in apoE$^{-/-}$ than in LDLR$^{-/-}$ mice, involvement of hyperlipidemia in food intake regulation might be unlikely in our model. Second, we speculate that leptin sensitization is involved in decreased food intake and increased energy expenditure. Obesity is well known to be associated with poor responses to leptin despite hyperleptinemia, a state defined as leptin resistance (32). Lower plasma leptin levels with lower body weight in apoE$^{-/-}$;Ay/+ mice compared with apoE$^{+/+}$;Ay/+ mice suggests greater leptin sentivity in the former. Therefore, decreased food intake and increased energy expenditure in apoE$^{-/-}$;Ay/+ mice might be explained by leptin sensitization. We have recently reported that alterations in metabolism in adipose tissue affect food intake amounts (19). However, *ob/ob*;apoE$^{-/-}$ mice are also reportedly resistant to obesity (14). Since *ob/ob* mice are leptin deficient, the obesity resistance in *ob/ob*;apoE$^{-/-}$ mice is not mediated by leptin signaling, e.g., leptin sensitization, although food intake and energy expenditure were not measured in the earlier study (14). Thus, mechanisms other than leptin sensitization might be involved in decreased food intake and increased energy expenditure in apoE$^{-/-}$;Ay/+ mice. Third, direct effects of apoE on neurons are also possible. ApoE, produced by glial cells, is a major apolipoprotein in the brain and mediates the transport of cholesterol and phospholipids, and its receptors are abundantly expressed on neurons (33). Furthermore, numerous studies have shown that apoE plays multiple roles in the nervous system. In the central and peripheral nervous systems, apoE promotes neurite outgrowth and regeneration (34). ApoE protects neurons from oxidative injury (35) and modulates amyloid-β deposition (36), interactions with Alzheimer amyloid precursor protein (37), and transmission of signals to neurons (38). In this context, modulation of neurons by apoE might be involved in energy metabolism. ApoE is reportedly expressed in tissues other than the liver, including the brain (33) and adipose tissue (39). ApoE deficiency in these tissues may affect the metabolic phenotypes of apoE$^{-/-}$;Ay/+ mice observed herein. Intensive research, including tissue-specific disruption of apoE or its receptor, is required to examine this hypothesis.

ApoE is involved in surplus fat accumulation and energy metabolism, including regulation of food intake and energy expenditure. Thus, excess fat accumulation via an apoE-dependent pathway might play a role in development of the metabolic syndrome. In addition to dissipation of surplus energy (4), apoE-dependent excess lipid transport is a potentially novel therapeutic target for the metabolic syndrome.

ACKNOWLEDGMENTS

This work was supported by a Grant-in-Aid for Scientific Research (B2, 15390282) to H.K.; a Grant-in-Aid for Scientific Research (17790599) to Y.I. from the Ministry of Education, Science, Sports and Culture of Japan; and a Grant-in-Aid for Scientific Research (H16-genome-003) to Y.O. from the Ministry of Health, Labor and Welfare of Japan. This work was also supported by the 21st Century COE Programs "CRESCENDO" to H.K. and "the Center for Innovative Therapeutic Development for Common Diseases" to Y.O. from the Ministry of Education Science, Sports and Culture.

We thank I. Sato, J. Fushimi, K. Kawamura, and M. Hoshi for technical support.

REFERENCES

1. Eckel RH, Grundy SM, Zimmet PZ: The metabolic syndrome. *Lancet* 365:1415–1428, 2005
2. Fruhbeck G, Gomez-Ambrosi J: Control of body weight: a physiologic and transgenic perspective. *Diabetologia* 46:143–172, 2003
3. Friedman JM: A war on obesity, not the obese. *Science* 299:856–858, 2003
4. Ishigaki Y, Katagiri H, Yamada T, Ogihara T, Imai J, Uno K, Hasegawa Y, Gao J, Ishihara H, Shimosegawa T, Sakoda H, Asano T, Oka Y: Dissipating excess energy stored in the liver is a potential treatment strategy for diabetes associated with obesity. *Diabetes* 54:322–332, 2005
5. Moitra J, Mason MM, Olive M, Krylov D, Gavrilova O, Marcus-Samuels B, Feigenbaum L, Lee E, Aoyama T, Eckhaus M, Reitman ML, Vinson C: Life without white fat: a transgenic mouse. *Genes Dev* 12:3168–3181, 1998
6. Shimomura I, Hammer RE, Richardson JA, Ikemoto S, Bashmakov Y,

Goldstein JL, Brown MS: Insulin resistance and diabetes mellitus in transgenic mice expressing nuclear SREBP-1c in adipose tissue: model for congenital generalized lipodystrophy. *Genes Dev* 12:3182–3194, 1998
7. Oral EA, Simha V, Ruiz E, Andewelt A, Premkumar A, Snell P, Wagner AJ, DePaoli AM, Reitman ML, Taylor SI, Gorden P, Garg A: Leptin-replacement therapy for lipodystrophy. *N Engl J Med* 346:570–578, 2002
8. Hussain MM, Maxfield FR, Mas-Oliva J, Tabas I, Ji ZS, Innerarity TL, Mahley RW: Clearance of chylomicron remnants by the low density lipoprotein receptor-related protein/alpha 2-macroglobulin receptor. *J Biol Chem* 266:13936–13940, 1991
9. Chappell DA, Medh JD: Receptor-mediated mechanisms of lipoprotein remnant catabolism. *Prog Lipid Res* 37:393–422, 1998
10. Cooper AD: Hepatic uptake of chylomicron remnants. *J Lipid Res* 38:2173–2192, 1997
11. Kuipers F, Jong MC, Lin Y, Eck M, Havinga R, Bloks V, Verkade HJ, Hofker MH, Moshage H, Berkel TJ, Vonk RJ, Havekes LM: Impaired secretion of very low density lipoprotein-triglycerides by apolipoprotein E-deficient mouse hepatocytes. *J Clin Invest* 100:2915–2922, 1997
12. Lyngdorf LG, Gregersen S, Daugherty A, Falk E: Paradoxical reduction of atherosclerosis in apoE-deficient mice with obesity-related type 2 diabetes. *Cardiovasc Res* 59:854–862, 2003
13. Schreyer SA, Vick C, Lystig TC, Mystkowski P, LeBoeuf RC: LDL receptor but not apolipoprotein E deficiency increases diet-induced obesity and diabetes in mice. *Am J Physiol Endocrinol Metab* 282:E207–E214, 2002
14. Chiba T, Nakazawa T, Yui K, Kaneko E, Shimokado K: VLDL induces adipocyte differentiation in ApoE-dependent manner. *Arterioscler Thromb Vasc Biol* 23:1423–1429, 2003
15. Zhang SH, Reddick RL, Piedrahita JA, Maeda N: Spontaneous hypercholesterolemia and arterial lesions in mice lacking apolipoprotein E. *Science* 258:468–471, 1992
16. Ishigaki Y, Oikawa S, Suzuki T, Usui S, Magoori K, Kim DH, Suzuki H, Sasaki J, Sasano H, Okazaki M, Toyota T, Saito T, Yamamoto TT: Virus-mediated transduction of apolipoprotein E (ApoE)-sendai develops lipoprotein glomerulopathy in ApoE-deficient mice. *J Biol Chem* 275: 31269–31273, 2000
17. Anai M, Funaki M, Ogihara T, Terasaki J, Inukai K, Katagiri H, Fukushima Y, Yazaki Y, Kikuchi M, Oka Y, Asano T: Altered expression levels and impaired steps in the pathway to phosphatidylinositol 3-kinase activation via insulin receptor substrates 1 and 2 in Zucker fatty rats. *Diabetes* 47:13–23, 1998
18. Usui S, Hara Y, Hosaki S, Okazaki M: A new on-line dual enzymatic method for simultaneous quantification of cholesterol and triglycerides in lipoproteins by HPLC. *J Lipid Res* 43:805–814, 2002
19. Yamada T, Katagiri H, Ishigaki Y, Ogihara T, Imai J, Uno K, Hasegawa Y, Gao J, Ishihara H, Niijima A, Mano H, Aburatani H, Asano T, Oka Y: Signals from intra-abdominal fat modulate insulin and leptin sensitivity through different mechanisms: neuronal involvement in food-intake regulation. *Cell Metab* 3:223–229, 2006
20. Uno K, Katagiri H, Yamada T, Ishigaki Y, Ogihara T, Imai J, Hasegawa Y, Gao J, Kaneko K, Iwasaki H, Ishihara H, Sasano H, Inukai K, Mizuguchi H, Asano T, Shiota M, Nakazato M, Oka Y: Neuronal pathway from the liver modulates energy expenditure and systemic insulin sensitivity. *Science* 312:1656–1659, 2006
21. Min J, Okada S, Kanzaki M, Elmendorf JS, Coker KJ, Ceresa BP, Syu LJ, Noda Y, Saltiel AR, Pessin JE: Synip: a novel insulin-regulated syntaxin 4-binding protein mediating GLUT4 translocation in adipocytes. *Mol Cell* 3:751–760, 1999
22. Takahashi S, Kawarabayasi Y, Nakai T, Sakai J, Yamamoto T: Rabbit very low density lipoprotein receptor: a low density lipoprotein receptor-like protein with distinct ligand specificity. *Proc Natl Acad Sci U S A* 89:9252–9256, 1992
23. Descamps O, Bilheimer D, Herz J: Insulin stimulates receptor-mediated uptake of apoE-enriched lipoproteins and activated alpha 2-macroglobulin in adipocytes. *J Biol Chem* 268:974–981, 1993
24. Wilsie LC, Chanchani S, Navaratna D, Orlando RA: Cell surface heparan sulfate proteoglycans contribute to intracellular lipid accumulation in adipocytes. *Lipids Health Dis* 4:2, 2005
25. Siri P, Candela N, Zhang YL, Ko C, Eusufzai S, Ginsberg HN, Huang LS: Post-transcriptional stimulation of the assembly and secretion of triglyceride-rich apolipoprotein B lipoproteins in a mouse with selective deficiency of brown adipose tissue, obesity, and insulin resistance. *J Biol Chem* 276:46064–46072, 2001
26. Fujino T, Asaba H, Kang MJ, Ikeda Y, Sone H, Takada S, Kim DH, Ioka RX, Ono M, Tomoyori H, Okubo M, Murase T, Kamataki A, Yamamoto J, Magoori K, Takahashi S, Miyamoto Y, Oishi H, Nose M, Okazaki M, Usui S, Imaizumi K, Yanagisawa M, Sakai J, Yamamoto TT: Low-density lipoprotein receptor-related protein 5 (LRP5) is essential for normal cholesterol metabolism and glucose-induced insulin secretion. *Proc Natl Acad Sci U S A* 100:229–234, 2003
27. Xu H, Barnes GT, Yang Q, Tan G, Yang D, Chou CJ, Sole J, Nichols A, Ross JS, Tartaglia LA, Chen H: Chronic inflammation in fat plays a crucial role in the development of obesity-related insulin resistance. *J Clin Invest* 112:1821–1830, 2003
28. Weisberg SP, McCann D, Desai M, Rosenbaum M, Leibel RL, Ferrante AW Jr: Obesity is associated with macrophage accumulation in adipose tissue. *J Clin Invest* 112:1796–1808, 2003
29. Takahashi S, Oida K, Ookubo M, Suzuki J, Kohno M, Murase T, Yamamoto T, Nakai T: Very low density lipoprotein receptor binds apolipoprotein E2/2 as well as apolipoprotein E3/3. *FEBS Lett* 386:197–200, 1996
30. Goudriaan JR, Tacken PJ, Dahlmans VE, Gijbels MJ, van Dijk KW, Havekes LM, Jong MC: Protection from obesity in mice lacking the VLDL receptor. *Arterioscler Thromb Vasc Biol* 21:1488–1493, 2001
31. Reaven GM: Banting lecture 1988: Role of insulin resistance in human disease. *Diabetes* 37:1595–1607, 1988
32. Considine RV, Sinha MK, Heiman ML, Kriauciunas A, Stephens TW, Nyce MR, Ohannesian JP, Marco CC, McKee LJ, Bauer TL, et al.: Serum immunoreactive-leptin concentrations in normal-weight and obese humans. *N Engl J Med* 334:292–295, 1996
33. Mahley RW, Nathan BP, Pitas RE: Apolipoprotein E: structure, function, and possible roles in Alzheimer's disease. *Ann N Y Acad Sci* 777:139–145, 1996
34. Masliah E, Mallory M, Ge N, Alford M, Veinbergs I, Roses AD: Neurodegeneration in the central nervous system of apoE-deficient mice. *Exp Neurol* 136:107–122, 1995
35. Chen Y, Lomnitski L, Michaelson DM, Shohami E: Motor and cognitive deficits in apolipoprotein E-deficient mice after closed head injury. *Neuroscience* 80:1255–1262, 1997
36. Bales KR, Verina T, Dodel RC, Du Y, Altstiel L, Bender M, Hyslop P, Johnstone EM, Little SP, Cummins DJ, Piccardo P, Ghetti B, Paul SM: Lack of apolipoprotein E dramatically reduces amyloid beta-peptide deposition. *Nat Genet* 17:263–264, 1997
37. Barger SW, Harmon AD: Microglial activation by Alzheimer amyloid precursor protein and modulation by apolipoprotein E. *Nature* 388:878–881, 1997
38. Trommsdorff M, Gotthardt M, Hiesberger T, Shelton J, Stockinger W, Nimpf J, Hammer RE, Richardson JA, Herz J: Reeler/disabled-like disruption of neuronal migration in knockout mice lacking the VLDL receptor and ApoE receptor 2. *Cell* 97:689–701, 1999
39. Zechner R, Moser R, Newman TC, Fried SK, Breslow JL: Apolipoprotein E gene expression in mouse 3T3–L1 adipocytes and human adipose tissue and its regulation by differentiation and lipid content. *J Biol Chem* 266:10583–10588, 1991

Efficient and controlled gene expression in mouse pancreatic islets by arterial delivery of tetracycline-inducible adenoviral vectors

Rui Takahashi, Hisamitsu Ishihara, Kazuma Takahashi, Akira Tamura, Suguru Yamaguchi, Takahiro Yamada, Hideki Katagiri[1] and Yoshitomo Oka

Division of Molecular Metabolism and Diabetes, Tohoku University Graduate School of Medicine, 2-1 Seiryo-machi, Aoba-ku, Sendai, Miyagi 980-8575, Japan

[1]Advanced Therapeutics for Metabolic Diseases, Center for Translational and Advanced Animal Research, Tohoku University Graduate School of Medicine, Sendai 980-8575, Japan

(Requests for offprints should be addressed to H Ishihara; Email: hisamitsu-ishihara@mail.tains.tohoku.ac.jp)

Abstract

Gene transfer with adenovirus vectors has been used extensively for pancreatic islet research. However, infection efficiency varies among reports. We reevaluated the infection efficiency, defined here as the percentage of islet cells expressing transgenes, in mouse islets. When the isolated islets were infected with adenoviruses, the infection efficiency was found to be 30–40% and the transduced cells were distributed in the islet periphery. Collagenase treatment of isolated islets before infection increased the infection efficiency to 70%, but with suppression of glucose-stimulated insulin secretion. To explore more efficient strategies, we employed arterial delivery of virus particles to islets *in situ*. Delivery of adenovirus ($\sim 10^8$ particles per pancreas) through the celiac and superior mesenteric arteries is highly efficient, resulting in more than 90% transduction without impairing glucose-stimulated insulin secretion. Arterial delivery of an adenovirus harboring glycerol kinase cDNA allowed us to observe glycerol-stimulated insulin secretion from mouse islets, which was not observed when we employed the conventional method. Furthermore, the arterial delivery method combined with a tetracycline-inducible adenovirus system induced efficient and controlled transgene expression. Our data provide new insights into gene transduction methods using recombinant adenoviruses in mouse islets, and are therefore anticipated to contribute to future basic and clinical islet research applications.

Journal of Molecular Endocrinology (2007) **38**, 127–136

Introduction

Gene therapy holds promise for the treatment of many human diseases, including diabetes mellitus (Yechoor & Chan 2005). *Ex vivo* gene transfer to pancreatic β-cells offers a potential means of preventing β-cell death via the expression of immunoregulatory, cytoprotective, or anti-apoptotic genes (Fernandes *et al.* 2004, Tran *et al.* 2004). In addition, the induction of transcriptional regulators and growth factors by gene therapy could stimulate β-cell differentiation and regeneration (Brun *et al.* 2004, Cozar-Castellano *et al.* 2004). Among several gene transfer vehicles, adenovirus vectors are attractive because they have the capacity for large DNA inserts, can be produced at high titers and have abilities to transduce non-dividing cells. In addition to potential therapeutic uses, adenovirus vectors are valuable experimental tools for genetic manipulation of islet cells. However, using adenovirus vectors, infection efficiency, defined here as the percentage of cells expressing transgenes, are reportedly variable, ranging from 10 to 80% in human (Giannoukakis *et al.* 1999, Leibowitz *et al.* 1999, Barbu *et al.* 2005, Rao *et al.* 2005), rat (Becker *et al.* 1994, Weber *et al.* 1997, Ishihara *et al.* 2003, Zhou *et al.* 2003, Diraison *et al.* 2004), and mouse (Csete *et al.* 1995, Bertera *et al.* 2003, Garcia-Ocana *et al.* 2003, Leclerc *et al.* 2004, Diao *et al.* 2005) islets.

There exist large numbers of genetically modified mice and basic aspects of mouse pancreatic islets have been intensively studied. Therefore, mouse islets are a suitable model for applying adenovirus technology, with the goal of clinical application of *ex vivo* gene transfer for this endocrine organ. For certain purposes, including transfection of cytoprotective genes for islet transplantation, it is essential that most of the cells express the transgenes. High efficiency is also desirable for studying islet biology and essential for suppressing gene expression in islets with adenovirus-mediated shRNA expression (Bain *et al.* 2004, Diao *et al.* 2005). In this study, we first reevaluated the transfection efficiency of recombinant adenoviruses in mouse islets and then explored the usefulness of different strategies, collagenase treatment before infection, and arterial delivery of virus particles *in situ*. We observed markedly improved infection efficiency with these methods. In particular, arterial delivery combined with a tetracycline-inducible

Journal of Molecular Endocrinology (2007) **38**, 127–136
0952-5041/07/038–127

DOI: 10.1677/jme.1.02189
Online version via http://www.endocrinology-journals.org

adenovirus system induced reliable and controlled expression of foreign genes in mouse islets.

Material and methods

Mouse

C57BL/6 mice, 12–16 weeks of age, were used. All animal experiments were approved by the Tohoku University Institutional Animal Care and Use Committee (#15–110).

Recombinant adenoviruses

AdRIP-HArGlyK expressing hemagglutinin (HA) epitope-tagged rat glycerol kinase under control of the rat insulin 1 promoter was described previously (Takahashi *et al.* 2006). The cytomegalovirus (CMV) promoter containing the Tet operator sequence (CTO) and the enhanced green fluorescent protein (eGFP) cDNA were excised from pcDNA5/TO (Invitrogen) and pEGFP-1 (BD Biosciences Clontech) respectively, and then ligated. The Tet-repressor cDNA was excised from pcDNA6/TR (Invitrogen) and ligated to the CAG promoter unit (Niwa *et al.* 1991). The CMV-eGFP expression unit was excised from pEGFP-1. These expression units were cloned into a cosmid vector pAdex1cw (Miyake *et al.* 1996). These cosmid vectors containing the expression units and adenovirus DNA-terminal protein complex were then co-transfected into HEK293 cells, which were then seeded onto 96-well plates. After 10 days, cytopathic effects were seen in several wells. Recombinant adenoviruses were extracted from 96-well plates and amplified first in HEK293 cells in 24-well plates and then in cells in 3×150 mm dishes. Usually, we pick up adenoviruses from 96-well plates in which no more than 20 wells show cytopathic effects. In addition, careful examination of adenovirus DNA structure by enzyme digestion excludes contamination with adenoviruses lacking some portion of their genome. Therefore, we consider the purity of the virus preparation to be similar to that obtained from purified plaques. Amplified adenoviruses were purified with CsCl gradient ultracentrifugation. The resulting viruses were designated AdCAG-TR for the Tet repressor expressing virus, AdCMV-eGFP for the eGFP-expressing virus under the CMV promoter, and AdCTO-eGFP for the eGFP-expressing virus under the CMV promoter with the Tet operator. Virus infectious titers (plaque-forming unit (pfu)) were determined by a previously described method (Miyake *et al.* 1996). Amounts of virus particles were calculated from OD260 with a formula in which 1 OD260 corresponds to $1{\cdot}1\times10^{12}$ particles/ml (Maizel *et al.* 1968). Viral particle to pfu ratios of these virus stocks were 20–80. Infectious titer (pfu) is more closely related to viral infectivity and thus used to present the virus amount in this study.

Isolation of mouse islets and infection with recombinant adenoviruses

Islets were isolated by retrograde infusion of 1·3 ml cold Hanks'-balanced salt solution containing 1·0 mg/ml collagenase (Sigma-Aldrich) from the common bile duct and harvested by hand under microscopy. One hundred islets, immediately after isolation or after overnight culture, were placed in 1 ml RPMI media containing 10% fetal bovine serum, 11 mM glucose, 100 U/ml penicillin, and 100 μg/ml streptomycin, to which recombinant adenoviruses were added at an m.o.i. of 300 (assuming 2500 cells per islet; $7{\cdot}5\times10^7$ pfu of viruses/100 islets per milliliter), and cultured at 37 °C for 2 h. Islets were then washed twice with the media and cultured for 48 h in RPMI media. In some of the experiments, islets cultured overnight were treated with 1 ml Hanks'-balanced salt solution containing 1·0 mg/ml collagenase for 10 min at 37 °C, washed twice with PBS and then infected with recombinant adenoviruses as mentioned earlier.

Arterial delivery of adenovirus vectors

For arterial delivery of virus particles, polyethylene tubes 0·3 mm in diameter were inserted into the celiac artery (CA) and the superior mesenteric artery (SMA) (Fig. 1). Viruses (0·5 to 5×10^8 pfu) were diluted in 1·3 ml saline. After clamping the portal vein and the hepatic artery as well as the splenic artery, an approximately 0·9 ml viral solution was injected into the pancreas via the CA and 0·4 ml through the SMA. The pancreas was left at room temperature for 10 min and then 1·3 ml cold Hanks'-balanced salt solution containing 1·0 mg/ml collagenase was infused through the common bile duct. Islets were harvested by hand and cultured for 48 h.

GFP expression and immunocytochemistry of islet sections

Islets were fixed with 4% paraformaldehyde for 15 min at 4 °C, immersed in 5% sucrose/PBS for 30 min and 30% sucrose/PBS for 1 h. Samples were then embedded in TISSU MOUNT (Chiba Medical, Saitama, Japan) and quick-frozen in liquid nitrogen. Islet sections (6 μm) were made using a cryostat and examined for eGFP fluorescence with a Leica fluorescent microscope (DFC350FX). Sections were also stained with anti-insulin and anti-glucagon antibodies (Sigma-Aldrich).

Flow cytometric analysis of GFP expression

The infected islet cells were quantitatively analyzed by flow cytometry (FACS Calibur; BD Bioscience Clontech) on at least 1×10^4 cells per sample. Forty-eight hours after infection, islet cells were dispersed by

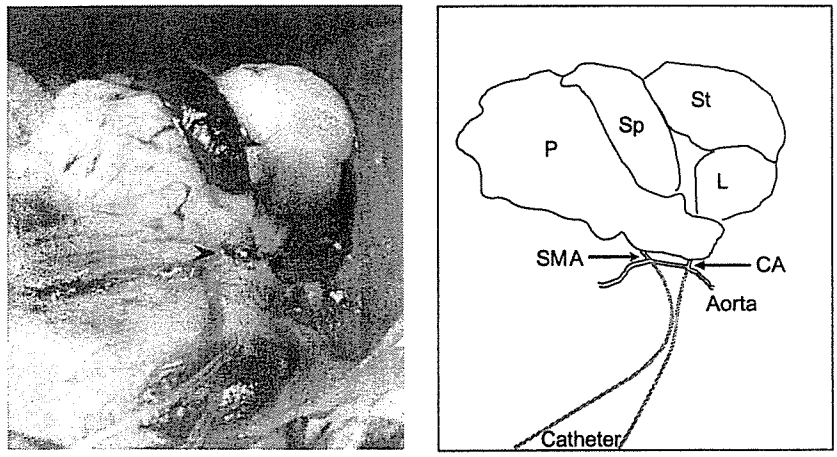

Figure 1 Arterial delivery of recombinant adenovirus into mouse pancreas. Polyethylene tubes 0·3 mm in diameter were inserted into the celiac artery (CA, triangle) and the superior mesenteric artery (SMA, arrowhead) at the points branching from the aorta. The pancreas (P) was infused with virus solution and thereby distended. Sp, spleen; St, stomach; L, liver.

treatment with 0·25% trypsin per 1 mM EDTA for 5 min at 37 °C. The percentage of eGFP-positive cells (in the M2 range) was determined after compensating for autofluorescence (in the M1 range) using uninfected cells as a negative control.

Measurement of insulin secretion

Islets (ten islets per tube) infected with recombinant adenoviruses were incubated over a period of 60 min in 1 ml Krebs–Ringer bicarbonate Hepes buffer (KRBH, 140 mM NaCl, 3·6 mM KCl, 0·5 mM NaH_2PO_4, 0·5 mM $MgSO_4$, 1·5 mM $CaCl_2$, 2 mM $NaHCO_3$, 10 mM Hepes (pH 7·4), 0·25% BSA) containing 2·5 mM glucose, 2·5 mM glucose plus 10 mM glycerol, 15 mM glucose or 20 mM glucose. Experiments were conducted with three to five tubes for each condition. Insulin was detected using RIA kits (LINCO, St Charles, MO, USA).

Statistical analysis

Data are presented as mean±S.E.M. when otherwise stated. Differences between groups were assessed by Student's *t*-test for paired or unpaired data.

Results

Adenovirus-mediated gene transfer using the conventional method

We reevaluated the efficiency of adenovirus infection in isolated mouse islets. An optimal titer of adenoviruses was first determined employing AdCMVeGFP expressing the enhanced Green fluorescent protein (eGFP). Analysis using a fluorescence-activated cell sorter (FACS) showed the percentage of islet cells expressing eGFP to be increased, as virus titer rose from multiplicity of infection (m.o.i.) of 100–900 (Fig. 2A). In addition, the expression levels, as evaluated by geometric mean fluorescence, were increased from 46·46±0·54 (m.o.i.=100), 71·98±5·79 (m.o.i.=300) to 111·26±6·56 (m.o.i.=900; arbitrary unit $n=3$). However, the infection of islets with AdCMV-eGFP at an m.o.i. of 900 resulted in reduced glucose (20 mM)-stimulated insulin secretion when compared with that in non-infected islets (data not shown), as was noted previously (Rao *et al.* 2005). In contrast, a more than fourfold increase in glucose-stimulated insulin secretion was observed in both non-infected islets and those infected with AdCMV-eGFP at an m.o.i. of 100 or 300 (data not shown). Therefore, for the subsequent studies, we used AdCMV-eGFP at an m.o.i. of 300.

Many other parameters affect infection efficiency, such as islet size and duration of exposure to the adenovirus. As described previously (Leclerc *et al.* 2004), we noticed that cells at the centers of islets with a diameter >150 μm were difficult to infect. Therefore, islets with a diameter between approximately 80 and 120 μm were employed for the present study. Very little necrosis of cells at the islet core (central necrosis) was seen in islets with this size range (data not shown). As to the duration of exposure to the adenovirus, we observed that 2-h exposure to the virus at 37 °C resulted in greater numbers of infected cells than 1-h exposure, while no further increases were seen with overnight exposure (data not shown).

Another factor that could affect the infection efficiency is the timing of adenovirus infection. Therefore, we examined whether overnight culture affects the infection efficiency in mouse islets. Islets were infected

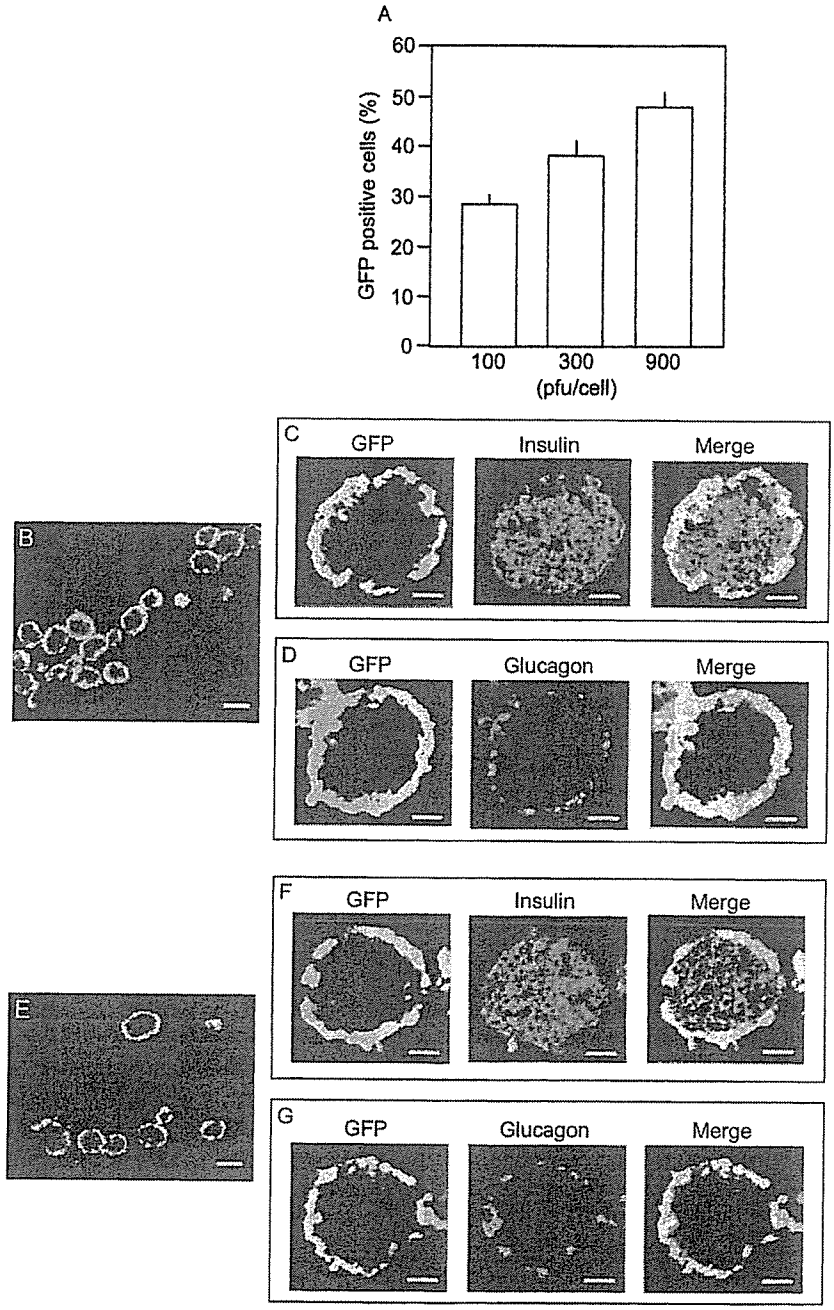

Figure 2 Adenovirus-mediated eGFP expression in mouse islets. (A) Mouse islets were infected with AdCMV-eGFP immediately after isolation at an m.o.i. of 100, 300, or 900. Percentages of eGFP-positive cells were analyzed by FACS 48 h after infection. Data are means±S.D. of three independent experiments. (B–D) Immunostaining of sections of mouse islets infected with AdCMV-eGFP (300 m.o.i.) immediately after isolation. Sections of islets were directly observed for eGFP at low magnification (×100) (B) or stained with anti-insulin (C) or anti-glucagon (D) and observed at high magnification (×400). (E–G) Immunostaining of sections of mouse islets infected with AdCMV-eGFP (300 m.o.i.) after an overnight culture. Sections of islets were directly observed for eGFP at low magnification (×100) (E) or stained with anti-insulin (F) or anti-glucagon (G) and observed at high magnification (×400). Bars, 100 μm in B and E, and 20 μm in C, D, F and G.

with AdCMV-eGFP either immediately after isolation or after an overnight culture. Some eGFP-positive cells were observed in the inner parts of islets when islets were infected immediately after isolation (Fig. 2B–D), while eGFP-positive cells were located almost exclusively in the surface layer of islets when infected after an overnight culture (Fig. 2E–G). Quantitative analysis using a FACS demonstrated that eGFP-positive cell numbers tended to be greater in islets infected immediately after isolation (39·8±2·4%, $n=3$) than in those infected after an overnight culture (35·6±1·2%, $n=3$), but the difference did not reach statistical significance. Immunostaining with an insulin or glucagon antibody revealed that small percentages of β-cells were infected either immediately after isolation (Fig. 2C) or after an overnight culture (Fig. 2F), while very high percentages of α-cells, nearly 100%, were infected. The latter observation was especially apparent in islets infected immediately after isolation (Fig. 2D and G).

Islets were fragmented or damaged with a few cells detaching from the islet surface immediately after isolation (data not shown). In contrast, islets appeared to have recovered, forming compact spheres, after an overnight culture. We speculated that the somewhat higher infection efficiency in islets immediately after isolation might be related to islet surface damage, which allows virus entry into the inner parts of islets.

Increased efficiency of adenovirus infection after collagenase treatment

To improve the infection efficiency, islets cultured overnight were treated with 1·0 mg/ml collagenase for 10 min at 37 °C before adenovirus infection. Infected islets are then cultured for 48 h. We observed eGFP-positive cells even at the islet center (Fig. 3A–C) and recognized a marked increase in the percentage of eGFP-positive cells; average infection efficiency was 73·24±5·30% ($n=3$). Representative data of the FACS analysis were shown in Fig. 3D. Consequently, not only α-cells, but also the majority of β-cells expressed eGFP (Fig. 3B and C). We also tested 0·2 and 0·5 mg/ml collagenase, but found efficiency to be lower than with 1·0 mg/ml collagenase (data not shown).

We first confirmed that insulin secretion was not affected by treatment with 1·0 μg/ml collagenase (Fig. 3E). We then studied the effects of adenovirus infection after collagenase treatment on glucose-stimulated insulin secretion. Glucose responsiveness was preserved as judged by similar ratios of stimulated over basal insulin secretion in control islets (5·27±0·50-fold, $n=3$) and islets infected with AdCMV-eGFP after collagenase treatment (5·29±0·81-fold, $n=3$; Fig. 3F). However, absolute amounts of insulin secreted from islets were significantly lower when islets were infected after collagenase treatment than those of non-infected and non-treated islets (Fig. 3F, open columns versus closed columns). The decrease in insulin secretion was not attributable to reduced insulin contents, since insulin contents did not differ between these islets (226·3±46·5 vs 228·5±35·4 ng/islet, $n=3$ experiments, for control and infected islets respectively). Considering that the fold-increase in glucose-stimulated insulin secretion and insulin content in infected islets were similar to those in non-infected islets, glucose-sensing, and the associated intracellular signaling were thought to be unaffected, while insulin exocytosis was impaired by adenovirus infection after collagenase treatment.

Arterial delivery of recombinant adenovirus increased gene transduction efficiency

Next, to devise a better infection method, we examined gene transduction efficiency with adenovirus delivery to mouse islets *in situ* through arteries perfusing the pancreas. Arterial delivery of recombinant adenoviruses has been used to infect islets of obese Zucker diabetic fatty rats (Wang *et al.* 1998). However, neither the details of the method used nor its infection efficiency have been described. Furthermore, arterial delivery has not been applied for mouse islet infection. Therefore, we tested the feasibility of delivering recombinant adenoviruses through both the celiac artery (CA) and the superior mesenteric artery (SMA). The SMA perfuses mainly the ventral portion of the pancreas, while the CA supplies the pancreatic body and tail. With the portal vein and the hepatic artery as well as the splenic artery clamped, $3·4\times10^8$ plaque forming units (pfu) of AdCMV-eGFP virus were delivered through these arteries: 70% through the CA and 30% through the SMA (Fig. 1). The pancreas was then left at room temperature for 10 min. The islets were next isolated by retrograde collagenase infusion through the common bile duct. More than 90% of islets showed viral infection with this method emitting green fluorescence (Fig. 4A). Importantly, eGFP-positive cells were distributed throughout almost all infected islets, and the intensity of green fluorescence was homogenous (Fig. 4A–C). Furthermore, both β-cells (Fig. 4B) and α-cells (Fig. 4C) were effectively infected. Quantitative assessment of efficiency, determined using FACS, revealed 90·37± 2·0% ($n=3$) of islet cells to be infected with the adenovirus. The expression levels of eGFP in individual cells were very high as shown by the rightward shift of the peak fluorescence in the FACS analysis (Fig. 4D compared with Fig. 3D). In addition, glucose-stimulated insulin secretion was unaffected by infection with adenovirus delivered through the CA and the SMA, being essentially the same as that in non-infected control islets (Fig. 4E).

We then studied the impact of rat glycerol kinase expression (rGlyK), by the arterial delivery method, on

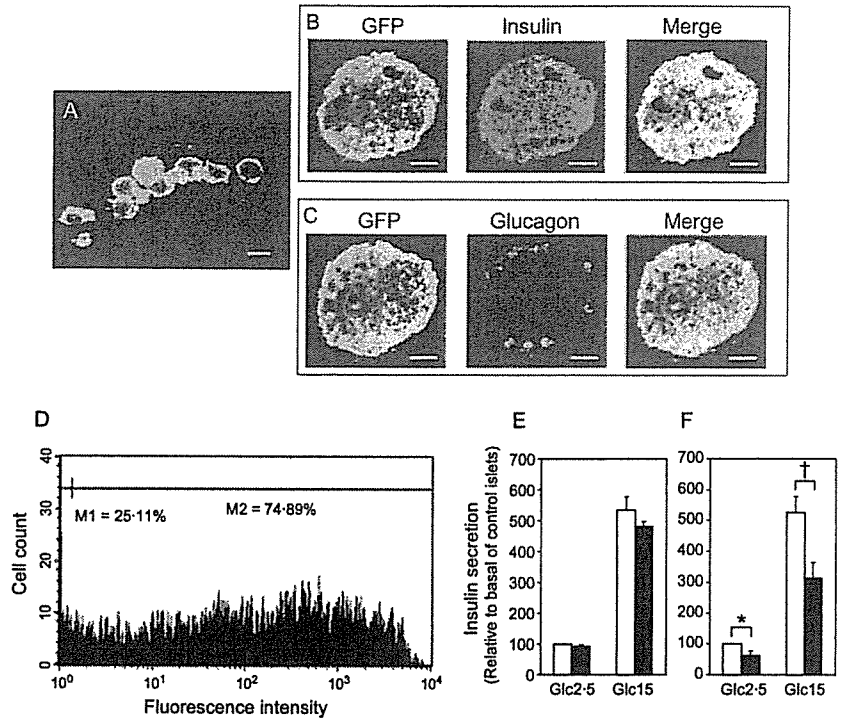

Figure 3 Effects of collagenase treatment on AdCMV-eGFP infection in overnight-cultured islets. (A–C) Immunostaining of sections of mouse islets infected with AdCMV-eGFP after collagenase treatment. Sections of islets were directly observed for eGFP at low magnification (×100) (A) or stained with anti-insulin (B) or anti-glucagon (C) and observed at high magnification (×400). Bars, 100 μm in A and 20 μm in B and C. (D) Flow cytometric analysis of eGFP-positive cells in islets infected after collagenase treatment. One representative result from three experiments is presented. (E) Glucose-stimulated insulin secretion from collagenase-treated islets (closed columns) and non-treated control islets (open columns). The value of insulin secretion from control islets at 2·5 mM glucose (6·54±0·72 ng/h per ten islets, n=3) was taken as 100%. Data are means±S.E.M. from three independent experiments. (F) Glucose-stimulated insulin secretion from islets infected with AdCMV-eGFP after an overnight culture with collagenase treatment (closed columns) and that of control islets, which were neither infected nor treated with collagenase (open columns). The values of insulin secretion from control islets at 2·5 mM glucose (7·01±0·64 ng/h per ten islets, n=3) was taken as 100%. Data are means±S.E.M. from three independent experiments. $^{*}P<0·05$, $^{\dagger}P<0·01$.

β-cell-secretory functions. We previously reported that glycerol stimulates insulin secretion from INS-1E cells and rat β-cells overexpressing rGlyK (Takahashi *et al.* 2006). However, when mouse islets were infected immediately after isolation with AdRIP-HArGlyK expressing rGlyK (Fig. 5A), we detected no glycerol-stimulated insulin secretion (Fig. 5B). We considered this to be due to low efficiency of adenovirus infection into mouse β-cells with the conventional method (Fig. 5A). Therefore, mouse islets were infected with AdRIP-HArGlyK via delivery through the CA and the SMA. When islets were infected with arterially delivered viruses, almost all β-cells expressed HA-GlyK (Fig. 5C). As expected, glycerol (10 mM) evoked insulin secretion from mouse islets infected with AdRIP-HArGlyK delivered through these arteries (Fig. 5D). These data, taken together, indicate that adenovirus administration through the CA and the SMA allows very high infection efficiency without adverse effects on islet-secretory activities.

Controlled gene expression with tetracycline-inducible adenoviruses

In comparing the effects of different adenovirus transductions, it is essential to use fixed amounts of adenoviruses, which do not differ between control and experimental groups. However, this is not an easy task. To create comparable conditions when using the arterial delivery method, a tetracycline-inducible system was applied. This system employs an adenovirus expressing the Tet repressor (AdCAG-TR) and another virus with a

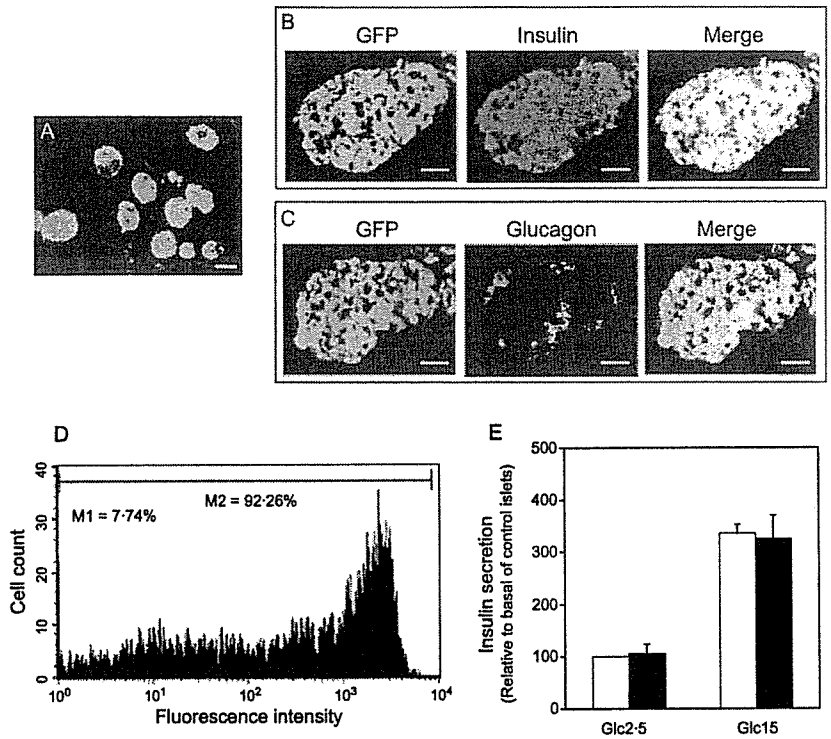

Figure 4 Efficient gene transduction through arterial delivery of adenovirus vectors. (A–C) Immunostaining of sections of mouse islets infected with AdCMV-eGFP delivered through the CA and the SMA. Sections of islets were directly observed for eGFP at low magnification (×100) (A) or stained with anti-insulin (B) or anti-glucagon (C) and observed at high magnification (×400). Bars, 100 μm in A and 20 μm in B and C. (D) Flow cytometric analysis of eGFP-positive cells in islets infected with AdCMV-eGFP delivered through the CA and the SMA. One representative result out of three is shown. (E) Glucose-stimulated insulin secretion from islets infected with AdCMV-eGFP delivered through the CA and the SMA (closed columns) and that of non-infected islets (open columns). The value of insulin secretion from control islets at 2·5 mM glucose (2·89±0·68 ng/h per ten islets, $n=3$) was taken as 100%. Data are means±S.E.M. from three independent experiments.

promoter containing the Tet operator. AdCTO-eGFP ($1{\cdot}5\times10^8$ pfu) expressing eGFP under control of the CMV promoter containing the Tet operator was delivered together with AdCAG-TR ($0{\cdot}5\times10^8$ pfu) into the pancreas through the CA and the SMA. Islets were then isolated, divided into two groups and incubated in media with or without doxycycline (2 μg/ml). Islets treated with doxycycline exhibited strong eGFP expression, while only weak expression in a limited number of cells was observed in islets infected with these viruses but not treated with doxycycline (Fig. 6). These data indicate that the arterial delivery method combined with the tetracycline-inducible system assure efficient and controlled gene expression in islets.

Discussion

We studied the effects of different infection methods on adenovirus infection efficiency in mouse islets, including virus delivery through the CA and the SMA. Several factors influence the efficiency of adenovirus infection and cause variable levels of cytotoxicity. Results should always be interpreted with caution, and limited infection efficiency and possible cytotoxicity must be taken into account.

The efficiency of adenovirus infection in pancreatic islets varies among reports. Since not all factors in previous studies were provided, reasons for the different efficiencies are unclear. In this study, we showed that collagenase treatment of islets before exposure to viruses improves the efficiency. High efficiencies in several studies (Becker *et al.* 1994, Giannoukakis *et al.* 1999, Ishihara *et al.* 2003, Zhou *et al.* 2003, Diao *et al.* 2005) could be due to surface damage by collagenase treatment during isolation. Necrosis of cells at the islet core (central necrosis) is sometimes observed and could affect infection efficiency (Ilieva *et al.* 1999, Giuliani *et al.* 2005). When efficiency is estimated by counting dispersed islet cells expressing transgenes, central necrosis could

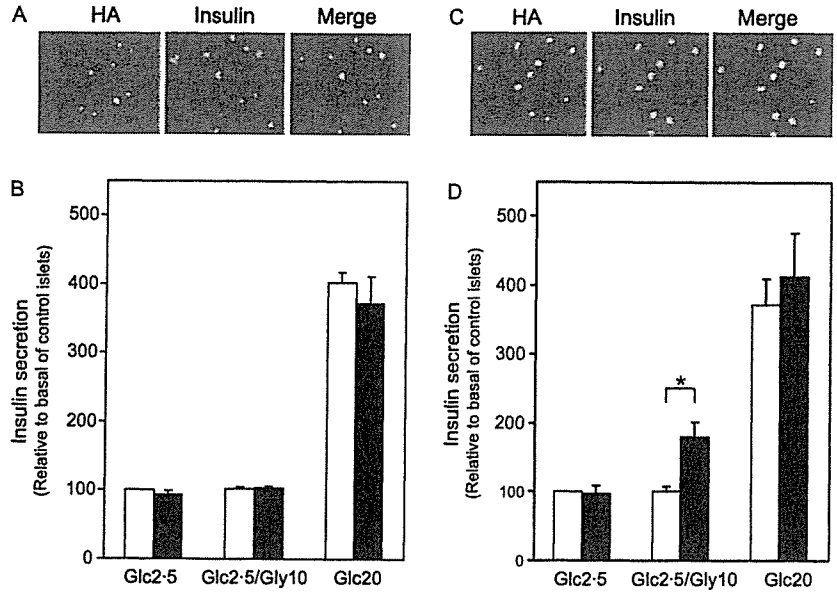

Figure 5 Impact of efficient gene expression, by arterial delivery of recombinant adenovirus, on insulin secretion. (A) Islets infected with AdRIP-HArGlyK immediately after isolation were cultured for 48 h, dispersed and stained with anti-HA or anti-insulin. Experiments were repeated thrice with essentially similar results. (B) Glucose (Glc; 20 mM) or glycerol (Gly; 10 mM)-stimulated insulin secretion from islets infected with AdRIP-HArGlyK immediately after isolation (closed columns) and non-infected control islets (open columns). The value of insulin secretion from control islets at 2·5 mM glucose (6·30±0·77 ng/h per ten islets, $n=4$) was taken as 100%. Data are means±S.E.M. from four independent experiments. (C) Islets infected with AdRIP-HArGlyK, delivered through the CA and the SMA, were cultured for 48 h, dispersed and stained with anti-HA or anti-insulin. Experiments were repeated twice with essentially similar results. (D) Glucose (20 mM) or glycerol (10 mM)-stimulated insulin secretion from islets infected with arterially delivered AdRIP-HArGlyK (closed columns) and non-infected control islets (open columns). The value of insulin secretion from control islets at 2·5 mM glucose (3·51±0·63 ng/h per ten islets, $n=3$) was taken as 100%. Data are means±S.E.M. from three independent experiments. *$P<0·05$.

result in an erroneous increase in efficiency. This is because there is a possibility that uninfected necrotic cells located in the islet core were lost during dispersion. Central necrosis occurs more often in relatively larger islets (Ilieva *et al.* 1999). In this respect, rat or human islets appear to be more susceptible to central necrosis than mouse islets. In mice, as demonstrated in this study using islets 80–120 μm in diameter, central necrosis is not a major problem.

Several methods have been employed to enhance adenoviral transgene expression. Adenoviruses enter cells via the coxsackievirus and adenovirus receptor (CAR). Use of a modified adenovirus that has an Arg-Gly-Asp (RGD) motif in the adenovirus fiber knob markedly improves infection efficiency in nonhuman primate isolated islets (Bilbao *et al.* 2002). We infected mouse islets with an eGFP-expressing adenovirus containing the RGD motif but observed no improvement in efficiency (R Takahashi, H Ishihara and H Mizuguchi, unpublished observation). Very high infection efficiency in monolayer culture of mouse islet cells suggests sufficient expression levels of CAR in mouse islet cells (Narushima *et al.* 2004). In addition, several agents were reported to enhance transgene expression in other cell types (Jornot *et al.* 2002, Huang *et al.* 2005, Triplett *et al.* 2005), and these agents may also be useful for pancreatic islet cells.

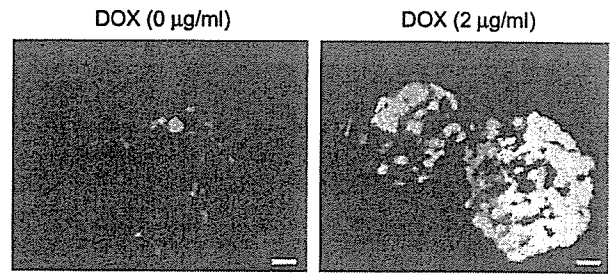

Figure 6 Doxycycline-inducible eGFP expression via adenoviruses delivered through the CA and the SMA. AdCAG-TR ($0·5\times10^8$ pfu) and AdCTO-eGFP ($1·5\times10^8$ pfu) were injected into the pancreas through the CA and the SMA. Expression of eGFP was induced by treatment with doxycycline (DOX, 2 μg/ml) for 48 h. The pictures shown are representative of three independent experiments. Bars, 20 μm.

Arterial delivery of adenovirus was demonstrated to be highly efficient, although the procedure is not as easy as infection of isolated islets *in vitro*. Since nearly 100% infection is not possible with conventional infection methods, this method could be useful when nearly 100% infection is desirable, such as gene silencing by expression of short hairpin RNA using adenoviral vectors. It is also likely that this method can be more easily applied to larger animals, including humans. In the present study, more than 90% infection was achieved by arterial delivery of approximately 3×10^8 (plaque forming units (pfu)) viruses. This is much less than the amount used in Zucker diabetic fatty rats (1×10^{12} pfu; Wang *et al.* 1998), even after taking into account the differences in animal sizes. The mouse pancreas contains more than 1000 islets, including small islets. On the assumption that average cell number in each islet is 1000 (not 2500 because of the presence of small islets), the administration of 3×10^8 viruses into a pancreas corresponds to an m.o.i. of 300. In fact, the m.o.i. in our experiments must have been <300, since the virus solution was distributed not only to islets but also to acinar cells. This might explain the lack of adverse effects on insulin secretion in association with virus infection by this method. Although the arterial delivery method is promising and the conditions we used in this study are acceptable in terms of the transfection efficiency, functional impact, and lack of adverse effects, further studies are needed to optimize conditions. In this regard, we found that the delivery of viruses at more than 3×10^9 pfu resulted in blunted glucose-stimulated insulin secretion and that more than 3 ml adenovirus solution cannot be infused when portal vein, hepatic artery, and splenic artery are clamped.

We also demonstrated combining arterial delivery of the virus with a tetracycline-inducible expression system to enhance the feasibility of the arterial delivery method. This method allows us to use exactly the same amount of adenovirus in the control and experimental groups, avoiding false results due to possible differences in titers of control and experimental viruses. As discussed in an earlier report (Irminger *et al.* 1996), there is inherent inaccuracy in determining adenovirus titers. The inducible adenovirus vector system is also advantageous since phenotype changes can be analyzed according to the degree of gain or loss of gene expression.

In conclusion, the present data provide new insight into gene transduction using recombinant adenoviruses in mouse islets. Our data demonstrate that adenovirus administration through the CA and the SMA yielded very high transduction efficiency in mouse islets. This method could easily be applied to human pancreas removed from donors prior to isolating islets. Several genes have been demonstrated to improve islet transplantation performance (Bertera *et al.* 2003, Garcia-Ocana *et al.* 2003, Fernandes *et al.* 2004). Our data could thus contribute to future studies in β-cell research, and may well be applicable to islet transplantation.

Acknowledgements

We thank Prof. T Ito (Tohoku University) for his helpful advice on the morphological studies. Dr A Gjinovci (University of Geneva) is greatly acknowledged for his advice on perfusion methodology. We are also grateful to Y Nagura and K Tanaka for their expert technical assistance.

Funding

This study was supported by a Grant-in-Aid for Scientific Research (17590264 to H I) and the 21st Century COE Programs ('the Center for Innovative Therapeutic Development for Common Diseases') to Y O from the Ministry of Education, Science, Sports and Culture of Japan. This work was also supported by a Grant-in-Aid for Scientific Research (H16-genome-003) to Y O from the Ministry of Health, Labor and Welfare of Japan. There is no conflict of interest that would prejudice the impartiality of any of the authors of this manuscript.

References

Bain JR, Schisler JC, Takeuchi K, Newgard CB & Becker TC 2004 An adenovirus vector for efficient RNA interference-mediated suppression of target genes in insulinoma cells and pancreatic islets of Langerhans. *Diabetes* **53** 2190–2194.

Barbu AR, Akusjarvi G & Welsh N 2005 Adenoviral-mediated transduction of human pancreatic islets: importance of adenoviral genome for cell viability and association with a deficient antiviral response. *Endocrinology* **146** 2406–2414.

Becker TC, BeltrandelRio H, Noel RJ, Johnson JH & Newgard CB 1994 Overexpression of hexokinase I in isolated islets of Langerhans via recombinant adenovirus. Enhancement of glucose metabolism and insulin secretion at basal but not stimulatory glucose levels. *Journal of Biological Chemistry* **269** 21234–21238.

Bertera S, Crawford ML, Alexander AM, Papworth GD, Watkins SC, Robbins PD & Trucco M 2003 Gene transfer of manganese superoxide dismutase extends islet graft function in a mouse model of autoimmune diabetes. *Diabetes* **52** 387–393.

Bilbao G, Contreras JL, Dmitriev I, Smyth CA, Jenkins S, Eckhoff D, Thomas F, Thomas J & Curiel DT 2002 Genetically modified adenovirus vector containing an RGD peptide in the HI loop of the fiber knob improves gene transfer to nonhuman primate isolated pancreatic islets. *American Journal of Transplantation* **2** 237–243.

Brun T, Franklin I, St-Onge L, Biason-Lauber A, Schoenle EJ, Wollheim CB & Gauthier BR 2004 The diabetes-linked transcription factor PAX4 promotes β-cell proliferation and survival in rat and human islets. *Journal Cell Biology* **167** 1123–1135.

Cozar-Castellano I, Takane KK, Bottino R, Balamurugan AN & Stewart AF 2004 Induction of beta-cell proliferation and retinoblastoma protein phosphorylation in rat and human islets using adenovirus-mediated transfer of cyclin-dependent kinase-4 and cyclin D1. *Diabetes* **53** 149–159.

Csete ME, Benhamou PY, Drazan KE, Wu L, McIntee DF, Afra R, Mullen Y, Busuttil RW & Shaked A 1995 Efficient gene transfer to pancreatic islets mediated by adenoviral vectors. *Transplantation* **59** 263–268.

Diao J, Asghar Z, Chan CB & Wheeler MB 2005 Glucose-regulated glucagon secretion requires insulin receptor expression in pancreatic α-cells. *Journal of Biological Chemistry* **280** 33487–33496.

Diraison F, Parton L, Ferre P, Foufelle F, Briscoe CP, Leclerc I & Rutter GA 2004 Over-expression of sterol-regulatory-element-binding protein-1c (SREBP1c) in rat pancreatic islets induces lipogenesis and decreases glucose-stimulated insulin release: modulation by 5-aminoimidazole-4-carboxamide ribonucleoside (AICAR). *Biochemical Journal* **378** 769–778.

Fernandes JR, Duvivier-Kali VF, Keegan M, Hollister-Lock J, Omer A, Su S, Bonner-Weir S, Feng S, Lee JS, Mulligan RC *et al.* 2004 Transplantation of islets transduced with CTLA4-Ig and TGFβ using adenovirus and lentivirus vectors. *Transplant Immunology* **13** 191–200.

Garcia-Ocana A, Takane KK, Reddy VT, Lopez-Talavera JC, Vasavada RC & Stewart AF 2003 Adenovirus-mediated hepatocyte growth factor expression in mouse islets improves pancreatic islet transplant performance and reduces beta cell death. *Journal of Biological Chemistry* **278** 343–351.

Giannoukakis N, Rudert WA, Ghivizzani SC, Gambotto A, Ricordi C, Trucco M & Robbins PD 1999 Adenoviral gene transfer of the interleukin-1 receptor antagonist protein to human islets prevents IL-1beta-induced beta-cell impairment and activation of islet cell apoptosis *in vitro*. *Diabetes* **48** 1730–1736.

Giuliani M, Moritz W, Bodmer E, Dindo D, Kugelmeier P, Lehmann R, Gassmann M, Groscurth P & Weber M 2005 Central necrosis in isolated hypoxic human pancreatic islets: evidence for postisolation ischemia. *Cell Transplantation* **14** 67–76.

Huang XW, Tang ZY, Lawrence TS & Zhang M 2005 5-Fluorouracil and hydroxyurea enhance adenovirus-mediated transgene expression in colon and hepatocellular carcinoma cells. *Journal of Cancer Research and Clinical Oncology* **131** 184–190.

Ilieva A, Yuan S, Wang RN, Agapitos D, Hill DJ & Rosenberg L 1999 Pancreatic islet cell survival following islet isolation: the role of cellular interactions in the pancreas. *Journal of Endocrinology* **161** 357–364.

Irminger JC, Meyer K & Halban PA 1996 Proinsulin processing in the rat insulinoma cell line INS after overexpression of the endoproteases PC2 or PC3 by recombinant adenovirus. *Biochemical Journal* **320** 11–16.

Ishihara H, Maechler P, Gjinovci A, Herrera PL & Wollheim CB 2003 Islet beta-cell secretion determines glucagon release from neighbouring alpha-cells. *Nature Cell Biology* **5** 330–335.

Jornot L, Morris MA, Petersen H, Moix I & Rochat T 2002 *N*-acetylcysteine augments adenovirus-mediated gene expression in human endothelial cells by enhancing transgene transcription and virus entry. *Journal of Gene Medicine* **4** 54–65.

Leclerc I, Woltersdorf WW, da Silva Xavier G, Rowe RL, Cross SE, Korbutt GS, Rajotte RV, Smith R & Rutter GA 2004 Metformin, but not leptin, regulates AMP-activated protein kinase in pancreatic islets: impact on glucose-stimulated insulin secretion. *American Journal of Physiology: Endocrinology and Metabolism* **286** E1023–E1031.

Leibowitz G, Beattie GM, Kafri T, Cirulli V, Lopez AD, Hayek A & Levine F 1999 Gene transfer to human pancreatic endocrine cells using viral vectors. *Diabetes* **48** 745–753.

Maizel JV Jr, White DO & Scharff MD 1968 The polypeptides of adenovirus. I. Evidence for multiple protein components in the virion and a comparison of types 2, 7A, and 12. *Virology* **36** 115–125.

Miyake S, Makimura M, Kanegae Y, Harada S, Sato Y, Takamori K, Tokuda C & Saito I 1996 Efficient generation of recombinant adenoviruses using adenovirus DNA-terminal protein complex and a cosmid bearing the full-length virus genome. *PNAS* **93** 1320–1324.

Narushima M, Okitsu T, Miki A, Yong C, Kobayashi K, Yonekawa Y, Tanaka K, Ikeda H, Matsumoto S, Tanaka N *et al.* 2004 Adenovirus mediated gene transduction of primarily isolated mouse islets. *ASAIO Journal* **50** 586–590.

Niwa H, Yamamura K & Miyazaki J 1991 Efficient selection for high-expression transfectants with a novel eukaryotic vector. *Gene* **108** 193–199.

Rao P, Roccisana J, Takane KK, Bottino R, Zhao A, Trucco M & Garcia-Ocana A 2005 Gene transfer of constitutively active Akt markedly improves human islet transplant outcomes in diabetic severe combined immunodeficient mice. *Diabetes* **54** 1664–1675.

Takahashi R, Ishihara H, Tamura A, Yamaguchi S, Yamada T, Takei D, Katagiri H, Endou H & Oka Y 2006 Cell type-specific activation of metabolism reveals that β-cell secretion suppresses glucagon release from α-cells in rat pancreatic islets. *American Journal of Physiology: Endocrinology and Metabolism* **290** E308–E316.

Tran PO, Parker SM, LeRoy E, Franklin CC, Kavanagh TJ, Zhang T, Zhou H, Vliet P, Oseid E, Harmon JS *et al.* 2004 Adenoviral overexpression of the glutamylcysteine ligase catalytic subunit protects pancreatic islets against oxidative stress. *Journal of Biological Chemistry* **279** 53988–53993.

Triplett JW, Herring BP & Pavalko FM 2005 Adenoviral transgene expression enhanced by cotreatment with etoposide in cultured cells. *Biotechniques* **39** 826–830.

Wang MY, Koyama K, Shimabukuro M, Newgard CB & Unger RH 1998 *OB-RB* gene transfer to leptin-resistant islets reverses diabetogenic phenotype. *PNAS* **95** 714–718.

Weber M, Deng S, Kucher T, Shaked A, Ketchum RJ & Brayman KL 1997 Adenoviral transfection of isolated pancreatic islets: a study of programmed cell death (apoptosis) and islet function. *Journal of Surgical Research* **69** 23–32.

Yechoor V & Chan L 2005 Gene therapy progress and prospects: gene therapy for diabetes mellitus. *Gene Therapy* **12** 101–107.

Zhou YP, Marlen K, Palma JF, Schweitzer A, Reilly L, Gregoire FM, Xu GG, Blume JE & Johnson JD 2003 Overexpression of repressive cAMP response element modulators in high glucose and fatty acid-treated rat islets. A common mechanism for glucose toxicity and lipotoxicity? *Journal of Biological Chemistry* **278** 51316–51323.

Received 19 September 2006
Accepted 6 October 2006

Endocrinology. First published ahead of print January 25, 2007 as doi:10.1210/en.2006-1351

TITLE

Bone Marrow (BM) Transplantation Promotes β Cell Regeneration after Acute Injury through BM Cell Mobilization

Abbreviated Title

BMT for β Cell Regeneration after Injury

AUTHORS

Yutaka Hasegawa[1,2†], Takehide Ogihara[1†], Tetsuya Yamada[2], Yasushi Ishigaki[2], Junta Imai[1,2], Kenji Uno[1,2], Junhong Gao[1,2], Keizo Kaneko[1,2], Hisamitsu Ishihara[2] Hironobu Sasano[3], Hiromitsu Nakauchi[4], Yoshitomo Oka[2] and Hideki Katagiri[1¶]

[1]Division of Advanced Therapeutics for Metabolic Diseases, Center for Translational and Advanced Animal Research, [2]Division of Molecular Metabolism and Diabetes, [3]Department of Pathology, Tohoku University Graduate School of Medicine, 2-1 Seiryo-machi, Sendai 980-8575 Japan, [4]Laboratory of Stem Cell Therapy, Center for Experimental Medicine, Institute of Medical Science, University of Tokyo, 4-6-1 Shirokanedai, Minato-ku, Tokyo 108-8639, Japan.

† These authors contributed equally to this work.

#Address correspondence to:

Hideki Katagiri, M.D., Ph.D.

Division of Advanced Therapeutics for Metabolic Diseases,

Center for Translational and Advanced Animal Research,

Tohoku University Graduate School of Medicine,

2-1 Seiryo-machi, Aoba-ku, Sendai 980-8575, Japan

Phone & Fax: +81-22-717-8228,

E-mail: katagiri@mail.tains.tohoku.ac.jp

Disclosure Statement: The authors have nothing to disclose.

Abstract

There is controversy regarding the roles of bone marrow (BM)-derived cells in pancreatic β cell regeneration. To examine these roles *in vivo*, mice were treated with streptozotocin (STZ), followed by bone marrow transplantation (BMT; lethal irradiation and subsequent BM cell infusion) from green fluorescence protein (GFP) transgenic mice. BMT improved STZ-induced hyperglycemia, nearly normalizing glucose levels, with partially restored pancreatic islet number and size, while simple BM cell infusion without pre-irradiation had no effects. In post-BMT mice, most islets were located near pancreatic ducts and substantial numbers of BrdU-positive cells were detected in islets and ducts. Importantly, GFP-positive, i.e. BM-derived, cells were detected around islets and were CD45-positive, but not insulin-positive. Then, to examine whether BM-derived cell mobilization contributes to this process, we used *Nos3*$^{-/-}$ mice as a model of impaired BM-derived cell mobilization. In STZ-treated *Nos3*$^{-/-}$ mice, the effects of BMT on blood glucose, islet number, BrdU-positive cells in islets and CD45-positive cells around islets were much smaller than those in STZ-treated *Nos3*$^{+/+}$ controls. A series of BMT experiments using *Nos3*$^{+/+}$ and *Nos3*$^{-/-}$ mice showed hyperglycemia-improving effects of BMT to correlate inversely with the severity of myelosuppression and delay of peripheral white blood cell recovery. Thus, mobilization of BM-derived cells is critical for BMT-induced β cell regeneration after injury. The present results suggest that homing of donor BM-derived cells in BM and subsequent mobilization into the injured periphery are required for BMT-induced regeneration of recipient pancreatic β cells.

INTRODUCTION

Several lines of evidence indicate that bone marrow (BM)-derived cells are capable of transdifferentiating into various cell types, including endothelial cells, arterial smooth muscle cells, myoblasts, myocardium and epithelia of the gastrointestinal tract (1-6). In the field of regenerative medicine for diabetes treatment, BM cells are seen as promising pancreatic β cell sources (7-9). However, whether BM cells can transdifferentiate into β cells and/or stimulate β cell differentiation is controversial.

A previous study showed that BM-derived cells can directly transdifferentiate into β cells (10). In that report, 4-6 weeks after BM transplantation (BMT; i.e. lethal irradiation of recipient mice and subsequent BM cell infusion from other mice), donor BM-derived insulin-positive cells were detected in 1.7-3% of pancreatic islet cells. However, in subsequent similar studies (11-13), very few or no donor BM-derived insulin-positive cells were detected in recipient islets, suggesting that, if direct transdifferentiation from BM-derived cells into β cells occurs, it would involve in only a very small percentage of cells. BM-derived cells also reportedly initiate recipient β cell regeneration rather than directly transdifferentiating into β cells (14). In that study, BMT increased recipient β cells with the appearance of donor-derived endothelial cells in the pancreas, resulting in improvement of hyperglycemia in streptozotocin (STZ)-induced diabetic mice. Other studies also demonstrated that BMT improves hyperglycemia in diabetic animals such as STZ-treated mice (15) and rats (16), E2f1/E2f2 mutant mice (17) and KKAy mice (18).

However, several studies obtained contradictory results, i.e. no improvement in hyperglycemia after BMT (12, 19). Whether BMT promotes β cell regeneration and improves hyperglycemia in diabetic mice and, if so, how β cells are regenerated remains essentially unknown. Herein, we attempted to address these questions.

First, we observed that BMT, but not simple BM cell infusion without pre-irradiation, restored islet numbers and improved hyperglycemia in STZ-treated mice. Donor-derived cells were detected around post-BMT islets and were CD45 (pan-hematopoietic marker)-positive, suggesting that mobilization of BM-derived cells to the pancreas induces β cell regeneration. To examine this hypothesis, we performed BMT experiments using endothelial nitric oxide synthase (eNOS)-deficient (*Nos3*$^{-/-}$) mice, in which mobilization of BM-derived cells after myelosuppression is impaired (20). In STZ-treated *Nos3*$^{-/-}$ mice, BMT effects on β cell regeneration and improvement of hyperglycemia were very limited. Thus, BM-derived cell mobilization is apparently involved in BMT-induced β cell regeneration after acute injury.

Experimental Procedures

Animals

C57BL/6J mice were purchased from Clea Japan, Inc (Tokyo, Japan). Green fluorescent protein (GFP) transgenic mice with the C57BL/6J background were kindly provided by Dr. M. Okabe (Osaka University) (21). Enhanced GFP is under transcriptional control of the chicken β-actin promoter and the cytomegalovirus enhancer in this strain, resulting in high-level expression in most tissues. *Nos3*$^{-/-}$ mice were purchased from Jackson Laboratories (Bar Harbor, ME). Age- and sex-matched wild-type (*Nos3*$^{+/+}$) littermates served as controls. These animals were generated and have been maintained with a C57BL/6J background by backcrossing of hemizygous carriers to C57BL/6J for >6 generations. Mice were housed in an air-conditioned environment, with a 12-h light-dark cycle, and fed a regular unrestricted diet. Hyperglycemia was induced by intraperitoneal infusion of 35 mg/kg body weight (BW) STZ (Sigma-Aldrich, St. Louis, MO) daily for 8 days (modification of method reported by Wang et al. (22)). STZ was solubilized in citrate sodium buffer (pH 4.5) and injected, within 15 min after preparation, into 6-week-old mice. All animal experiment procedures were approved by our Institutional Review Board, Tohoku University School of Medicine, and conducted according to institutional guidelines for animal experiments.

Measurements